CORONAL HOLE PROPERTIES OBSERVED WITH SUMER

K. STUCKI, S. K. SOLANKI, I. RÜEDI, J. O. STENFLO and A. BRKOVIĆ
Institute of Astronomy, ETH-Zentrum, CH-8092 Zürich, Switzerland

U. SCHÜHLE and K. WILHELM
Max-Planck-Institut für Aeronomie, D-37191 Katlenburg-Lindau, Germany

M. C. E. HUBER
European Space Agency, Space Science Department, ESTEC, PO Box 299, 2200 AG Nordwijk, The Netherlands

Abstract. We analyze SUMER spectra of 14 lines belonging to 12 ions, obtained on both sides of the boundary of polar coronal holes as well as at other locations along the limb. We compare line intensities, shifts and widths in coronal holes with values obtained in the quiet Sun. We find that with increasing formation temperature, spectral lines show an increasingly stronger blueshift in coronal holes relative to the quiet Sun at an equal heliospheric angle. The width of the lines is generally larger (by a few km/s) inside the coronal hole. Intensity measurements show the presence of the coronal hole in Ne VIII lines as well as in Fe XII, with evidence for a slightly enhanced emission in polar coronal holes for lines formed below 10^5 K.

1. Introduction

Coronal holes are the source of the fast solar wind and the primary example of coronal heating in regions with an excess of one magnetic polarity, but are not yet well understood. SUMER on board SOHO provides us with the capability of observing full line profiles at high spatial resolution, and thus determining line intensities, flows, and turbulent velocities in the chromosphere, transition region, and lower corona.

Distinctive differences in the center-to-limb intensity variations of lines between coronal holes and quiet Sun regions have been reported earlier by, e.g., Wilhelm *et al.* (1998). Here, we report on a comparison of high spatial and spectral resolution data of coronal hole and quiet Sun regions by comparing Gaussian-fit parameters of spectral lines measured at different locations along the limb.

2. Observations

Three sets of observations from SUMER were used. The first set consists of a series of 14 different spectral frames, each frame exposed for 300 seconds using the $1'' \times 300''$ slit placed on the central meridian. This slit crossed either the northern or the southern coronal hole (JOP055). The second set is very similar to the first one, but was taken 10 months later when the solar rotation compensation could be used (JOP055-TR).

The third set consists of a series of 12 different spectral frames taken during one of SOHO's roll maneuvers at different locations along the limb, with emphasis on the equator (slit $1'' \times 300''$, exposure time 150 s).
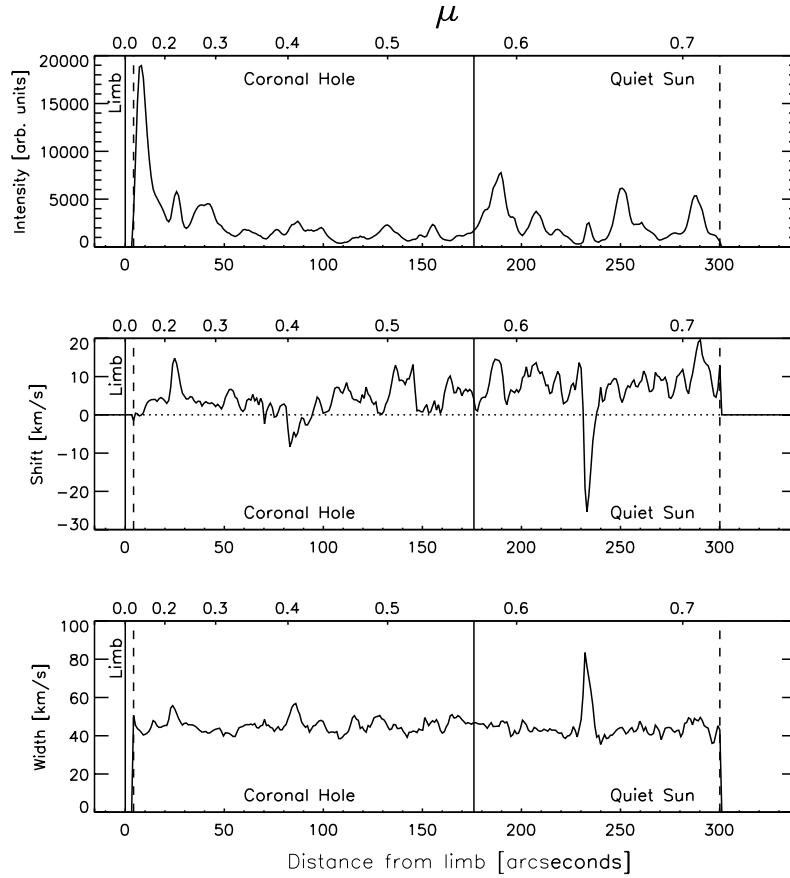
Figure 1. Example of the fit parameters (intensity, shift and width) using the spectral profiles of S VI at 933.39 Å, obtained from the first set of observations with SUMER (JOP055). The coronal hole boundary is located approximatively $176''$ from the limb (vertical line). The vertical line (solid line on the left) representing the position of the limb is located just outside the limits of the image on the detector (dashed vertical lines) in this data set. The scale at the top of each frame indicates $\mu = \cos \vartheta$, where ϑ is the heliocentric angle. The increased width near $230''$ marks the presence of an explosive event. Negative shifts signify blue shifts.

A group of spectral lines common to all observations was selected, and the intensity, shift, and width parameters were calculated at each spatial pixel using a Gaussian fitting method. The selected lines belong to: Si I, O I, N I, C II, Ni II, Si III, Si IV, N IV, O V, S VI, Ne VIII, and Fe XII. An example of the variation of line parameters along the slit is shown in Figure 1 for S VI 933.39 Å.

3. Results

In total we had about 25 exposures of each spectral line at our disposal. In each exposure, we averaged the fit parameters in a sector corresponding to the position
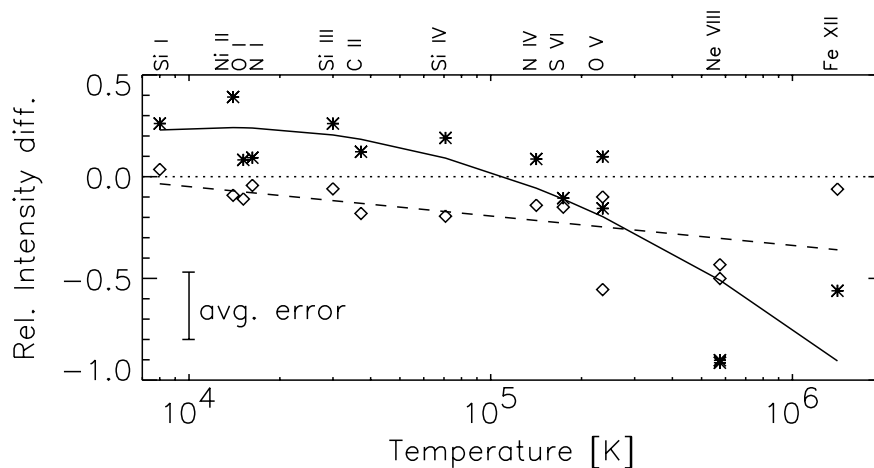
Figure 2. Relative intensity difference vs. ion temperature. The relative intensity difference was calculated using the expression: $2 \cdot (I_{\text{meridian}} - I_{\text{other locations}})/(I_{\text{meridian}} + I_{\text{other locations}})$. *Diamonds*: large μ sector (only quiet Sun); *Stars*: small μ sector (including coronal hole). The solid line shows a second order fit of the small μ sector points, while the dashed line shows a first order fit of the large μ sector points.

of the coronal hole ("small μ sector"), and in a sector corresponding to the quiet Sun ("large μ sector"). Those values were then averaged over all exposures taken at the meridian (containing northern or southern coronal hole regions), and over all exposures taken at other locations (roll data taken around the disk). The line parameters found are then related to the temperatures of maximum abundance of the ions taken from Arnaud and Rothenflug (1985).

In Figure 2 we plot the relative intensity difference between the meridian and the other locations, once for the "small μ sector" (stars) and once for the "large μ sector" (diamonds). The "small μ sector" consists of coronal hole data at the meridian and quiet Sun data at the other locations, while the "large μ sector" consists of quiet Sun data in all regions. Only the high temperature lines Ne VIII and Fe XII show reduced emission in the coronal hole. The large μ sector, which is outside the hole for every location, shows a smaller emission for the meridian data. The reason for this behavior is unknown. The influence of the FIP effect is currently being examined. Element fractionation is not apparent, possibly because it is covered by other effects.

The line shift displays a distinct trend towards larger blueshifts for higher ion temperatures in the coronal hole, which may be evidence of solar wind outflow at low altitudes in coronal holes (see Figure 3).

Figure 4 shows slightly increased line widths in the coronal hole, indicating higher non-thermal velocities for almost all lines except for Fe XII. The apparently contradictory result for Fe XII could be due to blends from cooler ions in its wings, which may contribute to its anomalous behavior.
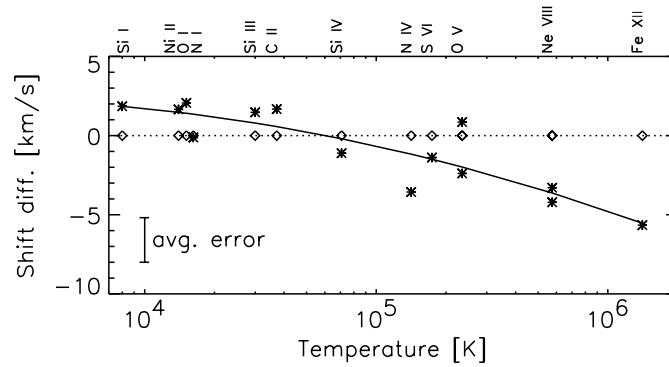
Figure 3. Wavelength shift difference in velocity units vs. formation temperature. The "shift differ-ence" represents the difference between the shifts observed on the meridian and the ones observed at other locations at the same μ. Since the wavelength scale is not absolute, we equalized the shifts between meridian and equator outside the hole. *Diamonds*: large μ sector (identically zero due to shift equalization); *Stars*: small μ sector (i.e., shift of hole profiles relative to non-hole profiles). The solid curve shows a second order fit of the small μ sector points.
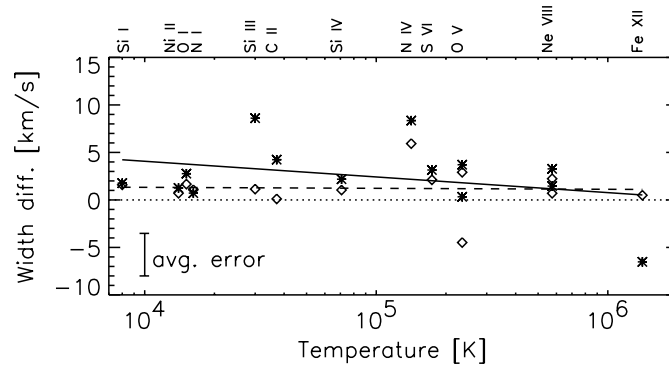

Figure 4. Width difference vs. formation temperature. The "width difference" represents the difference between the line width observed on the meridian and that at other locations. *Diamonds*: large μ sector; *Stars*: small μ sector (i.e., widths of hole profiles relative to non-hole profiles). The solid line shows a first order fit of the small μ sector points, while the dashed line shows a fit of the large μ sector points.

Acknowledgements

References

Arnaud, M., and Rothenflug, R.: 1985, *A&A,* **60**, 425.
Wilhelm, K., Lemaire, P., Dammasch, I. E., Hollandt, J., Schühle, U., Curdt, W., Kucera, T., Hassler, D. M., and Huber, M. C. E.: 1998, *A&A,* **334**, 685.